UJEAS

UNIZIK JOURNAL OF ENGINEERING AND APPLIED SCIENCES

UNIZIK Journal of Engineering and Applied Sciences 6(2), June (2026), 3404-3424
Journal homepage: https://journals.unizik.edu.ng/index.php/ujeas
PRINT ISSN: 2992-4383 || ONLINE ISSN: 2992-4391

Fretting wear mitigation: development of wear-resistant coconut shell particulate/aluminium composite

Paul Okpala[1*], Sam Omenyi[2], Ugochukwu Okonkwo[2], Jeremiah Chukwuneke[2], and Jude Dara[2]
[1]Department of Mechanical Engineering, Madonna University, Nigeria
[2]Department of Mechanical Engineering, Nnamdi Azikiwe University, Awka, Anambra State.
[*]Corresponding Author's E-mail: shalompaul2006@yahoo.com

Abstract
Fretting wear has remained a dominant problem in engineering, and efforts geared towards its mitigation have continued to gain attention within the research community. One of the ways of solving problems of fretting wear is through the design and development of wear-resistant materials, of which aluminium matrix composites are the material employed in this research. Aluminium matrix composites (AMCs) are widely employed in engineering applications requiring high strength-to-weight ratios; however, their mechanical and tribological performances are highly dependent on reinforcement strategy. This study presents a comprehensive evaluation of the mechanical and tribological properties of aluminium matrix composites incorporating carbonised coconut shell particulate reinforcement, using Response Surface Methodology (RSM) as an optimisation framework. Unreinforced aluminium alloy was included as a control sample to establish baseline mechanical and tribological behaviour. Ultimate tensile strength (UTS) and hardness were evaluated as key mechanical responses, while wear rate served as a tribological response. Results demonstrated that reinforcement significantly enhances mechanical and tribological performances relative to the control sample. The UTS values ranged from 42.907 to 74.403 MPa, with maximum strength observed at 212 µm particle size, 15 wt% reinforcement, and 2 minutes of stirring. Hardness reached 190.25 LHN, while wear rate decreased to 0.0055 mm³/m for the composite with 75 μm, 15 wt% and 5 min stirring time, demonstrating the positive effect of reinforcement on load-bearing capacity and wear resistance. Compared to pure aluminium, the composite improved UTS by up to 62%, hardness by up to 38%, reduced wear by up to 71%, and mitigated against fretting wear by 15%.

Keywords: Fretting Wear, Aluminium Matrix Composite (AMC), Mechanical Properties, Tribological Performance, Mitigation Factor.

1. Introduction

In tribology, fretting is a small oscillatory motion between contact surfaces (Yue and Wahab, 2019). And it occurs when two contacting surfaces exhibit a relative sliding motion between each other (Fantetti et al., 2019). Zhu et al. (2023) viewed fretting wear as the relative motion between contact surfaces with very small amplitude (displacement amplitude is usually in the order of microns) under the action of alternating loads such as mechanical vibration, fatigue load, electromagnetic vibration, fluid-induced vibration or thermal cycling. The wear associated with this small-amplitude relative oscillatory movement is known as fretting wear, which can involve both the abrasive and adhesive wear types. It is well known that fretting wear is the major cause for failure of mechanical components in modern industries, and it has become a major cause for concern to design and material engineers because of the catastrophic and costly nature of the damages caused by these failures. This damage, caused by fretting wear, incurs heavy losses on industries through the repair of the damaged parts and, in some cases, through outright replacement of the damaged parts. And it must be noted that this damage, for many machine parts, occurs after a very small percentage of the total volume has been worn out, which is the direct consequence of fretting wear.

Hence, components like bolts and nuts, pipes, bearings, keys and keyways, shafts, couplings, pistons and cylinders, etc., are expected to be made with wear-resistant materials for optimal life expectancy of such components during

their service life. Consequently, engineering material design and development will continue to gain centre stage in efforts geared towards the manufacture of wear-resistant material (Okpala et al., 2025).

Among various metal materials used for tribological applications, aluminium and its alloys are one of the most commonly studied. However, these types of materials are characterised by low hardness and limited tribological properties, which, in turn, limit the possibilities of their application (Almomani et al., 2020). The most popular way to increase the strength of aluminium and its alloys is to add insoluble reinforcement to create a metal matrix composite. Both monolithic (single reinforcement) and hybrid (more than one reinforcement in composite) composites could be developed, and in both cases, satisfactory results can be obtained in terms of tribological performance (Sydow et al., 2021). The most commonly used reinforcements for the aluminium matrix composite (AMC) are silicon carbide (SiC) and aluminium oxide (Al_2O_3) (Ramnath et al., 2014). But this study used agro waste (coconut shell) due to its availability and cost-effectiveness. Dara (2021) also confirmed the use of agro waste as a better and more cost-effective alternative to the more expensive synthetic reinforcements. Sydow et al. (2021) observed that waste management is still one of the leading global challenges in the 21st century. The reuse of waste for the production of tribological materials gives not only environmental benefits related to the transformation of waste into raw materials but also improves the mechanical and tribological properties of such materials.

Over the years, engineers have combated the menace of fretting wear through the use of lubricants. Zhang et al. (2023), for instance, investigated the low-temperature fretting wear behaviour of four commercial greases for use in wind turbine applications. Their work focused mainly on the use of lubrication for the mitigation of fretting wear in mechanical components; in this case, wind turbines, without any mention of material development for the mitigation of fretting wear. Yue et al. (2025) also studied the fretting and sliding composite wear behaviour of Ni-Al bronze under seawater lubrication. They paid attention to seawater lubrication, neglecting wear-resistant material development as a viable means of combating fretting wear.

From the extensive literature reviewed, there are few literature on fretting wear mitigation through the development of wear-resistant AMC. This is the gap that this research intends to bridge. This research, which is on the design and development of wear-resistant AMC for the mitigation of fretting wear, also developed a quantitative means of evaluating fretting wear mitigation, known as Mitigation Factor (MF) which serves as the novelty of the current study. Materials with higher mitigation factor will perform better than those with lower mitigation factor. The current study provides the basis for this evaluation. It aims to provide a systematically optimised evaluation of mechanical and tribological performance in reinforced aluminium matrix composites, explicitly incorporating an unreinforced aluminium alloy as control sample. This approach allows direct quantification of mechanical and tribological enhancement due to reinforcement, thereby strengthening the scientific basis of the findings.

2.0 Materials and methods

2.1 Materials

The aluminium alloy (Figure 1) was sourced from Cutix Plc, Nnewi, Anambra State, South East Nigeria and the coconut shell (Figure 2) was sourced from New Market in Enugu, Enugu State, South East Nigeria.

2.2 Thermal Analysis and optical micrograph of the Coconut Shell Particles

About 2 mg of 100 μm matured coconut shell particles were analysed at PGE Applied Resources Materials Laboratory. The TA instrument thermographic analyser TGA 2950 was used. This analysis showed the percentage weight change of the cocoanut shell particles with temperature, as shown in Figure 3. The graph depicts about four decomposition stages for the coconut shell particulate, but the final decomposition took place beyond the 650℃. The TGA revealed the stability of carbonized coconut shell particulates as reinforcement particles for aluminum, which melts at about a temperature of 660℃.

The result of the optical micrograph of the cocoanut shell particles given in Figure 4 revealed sharp and angular shape fragments with no spherical-shaped particles present. This is possibly due to the method used for the pulverisation of the coconut shell particulates, namely mechanical milling using mortar and piston. This shape has the advantage of increasing the mechanical interlocking with the aluminum matrix



Fig 1: Aluminum Cables



Fig 2: Coconut Shells

2.3 **Carbonisation and Sieving of the Coconut Shell Particles**

The coconut shell was washed with detergent to remove dirt and contaminants. It was rinsed in a clean bath of water and sun-dried for three days. The coconut shell was heated in a furnace to a temperature of 750℃ for 2 hours in an inert atmosphere to prevent combustion at the Scientific Equipment Development Institute (SEDI) Enugu. The carbonised cocoanut shells were allowed to cool down naturally in the furnace for three days. It was later pulverised and sieved into 75µm, 143.5µm and 212µm sized particulates in line with the design of experiment as shown in Figure 5.

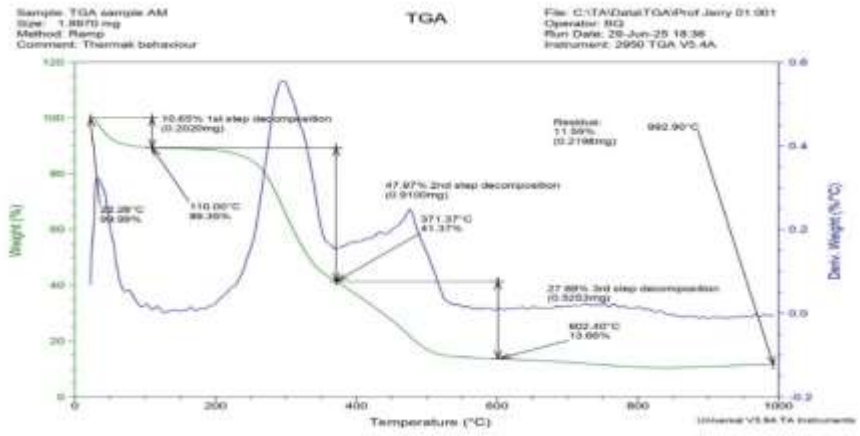

Fig 3: TGA/DTA Test Result

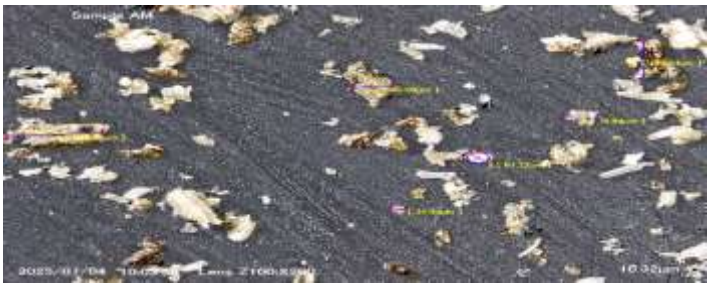

Figure 4: Optical Micrograph of Cocoanut Shell Particulates





75µm 143.5µm 212µm

Fig 5: 75µm, 143.5µm and 212µm sizes of carbonized cocoanut shells Particulates

2.4 Experimental Design

The design matrix is given in Table 1. The input parameters used for the produced composite sample include particle reinforcement size, particle weight percentage, and stirring time. The particulate reinforcement sizes were 75µm, 143.5µm and 212µm. The selected percentage weights are 5 wt%, 10 wt% and 15 wt%. The third chosen parameter is the stirring time. The selected stirring time were 2 minutes, 3.5 minutes and 5 minutes. The expected responses are the ultimate tensile strength (N/mm^2), hardness (LHN) and wear rate (mm^3/m).

Table 1: Design of Experiment

Sample	Factor 1: Particle Reinforcement Size ($\boldsymbol{\mu m}$)	Factor 2: Percentage Weight (%wt)	Factor 3 Stirring time (Mins)	Response 1: Ultimate Tensile Strength (MPa)	Response 2: Hardness (LHN)	Response 3: Wear Rate (mm^3/m)
1	75	5	5			
2	75	10	3.5			
3	75	15	2			
4	143.5	10	5			
5	212	15	5			
6	143.5	5	3.5			
7	212	5	5			
8	143.5	15	3.5			
9	212	10	3.5			
10	143.5	10	2			
11	75	5	2			
12	75	15	5			
13	212	5	2			
14	212	15	2			

2.5 Composite Production

Using stir casting method, the aluminium cable was heated to its molten form, and the reinforcement particulates were added and stirred mechanically for even distribution, in line with the design of experiment of Table 1. This was carried out at the foundry unit of Scientific Equipment Development Institute (SEDI), Enugu. The permanent mould ($120mm \times 20mm \times 8mm$) was preheated to avoid thermal shock when the molten composite was poured. Pure aluminium without reinforcement was first of all produced, and later the composites were produced in line with the parameters of the design of experiment, as observed in Figure 6. The produced composites were prepared and cut into samples for mechanical and tribological tests.



Fig 6: Cross section of the Produced Composite

2.6 Mechanical and Tribological Tests

Hardness and tensile tests were conducted at the laboratory of the Department of Metallurgical and Material Engineering, University of Nigeria, Nnsukka. The hardness test was done with a Leeb hardness tester (Figure 7). The device consist of a piston and ball with handle that strikes the surface of the material to be tested and an electronic interface that records the result in Leeb hardness number (LHN). The ball was stroke on four different surface, and the average was taken as the hardness of the sample.

All the samples were subjected to a tensile test using Testomeric Tensile testing Apparatus at Metallurgical and Material Engineering Laboratory, University of Nigeria Nsukka (UNN), with model number M 500-25CT and serial number 52978 (Figure 8). The machine has a gripping section where the sample is securely fixed and an electronic interface where the command is issued and the result displayed. All the results were noted down.

The wear behaviour of the samples were evaluated using a dry sliding pin-on-disc wear test, conducted at the Engineering laboratory of Standard Organization of Nigeria (SON), Enugu, as shown in Figure 9. After 300 revolutions of the rotating disc which were completed in 10 minutes 27 seconds, the weights of the samples were recorded before and after the test. Using equations 2 to 4, the sliding distance for each sample was computed and recorded.

$$angular\ velocity\ \omega = \frac{2\pi N}{60} \qquad (2)$$

$$angular\ displacement\ \theta = \omega t \qquad (3)$$

$$Sliding\ distance\ s = r\theta \qquad (4)$$

Wear rate was then determined using Khan et al.'s (2022) equation for calculating wear rate.

$$W_R = \frac{W_i - W_f}{\rho \times s} \qquad (5)$$



Fig 7: Leeb Hardness Tester



Fig 8: Tensile Testing Apparatus with Electronic Interface





Fig 9: Wear Test Apparatus

3.0 Result and Discussion

3.1 Hardness test Results

The hardness test result for the pure unreinforced aluminium is given in Table 2, while Table 3 gives the hardness values for the different compositions of the composites. Figure 10 showed improvement in hardness values for all the compositions of the reinforced composite. Composition 12 with input parameters of 75 μm, 15 wt% and 5 min stirring time gave the best hardness of 190.25 LHN against the 137.75 LHN of the unreinforced aluminium alloy, which is a significant 38.11% improvement in the hardness property.

Table 2: Hardness Value for the Unreinforced Aluminium (Okpala, 2026)

Sample	Test 1 (LHN)	Test 2 (LHN)	Test 3 (LHN)	Test 4 (LHN)	Average Hardness (LHN)
Aluminium Alloy	130	162	118	141	137.75

Table 3: Hardness Values for the Reinforced Composite (Okpala, 2026)

Sample	Test 1 (LHN)	Test 2 (LHN)	Test 3 (LHN)	Test 4 (LHN)	Average Hardness (LHN)	Improved Hardness (%)
1	188	133	151	139	152.75	10.89
2	121	154	163	126	141	2.36
3	161	188	122	169	160	16.15
4	155	122	186	123	146.5	6.35
5	145	169	118	151	145.75	5.80
6	154	215	108	184	165.25	19.96
7	127	189	157	183	164	19.06
8	204	188	147	171	177.5	28.86
9	131	232	158	162	170.75	23.96
10	135	182	136	206	164.75	19.60
11	161	135	204	118	154.5	12.16
12	145	154	213	249	190.25	38.11
13	107	152	192	127	144.5	4.9
14	122	181	165	151	154.75	12.34

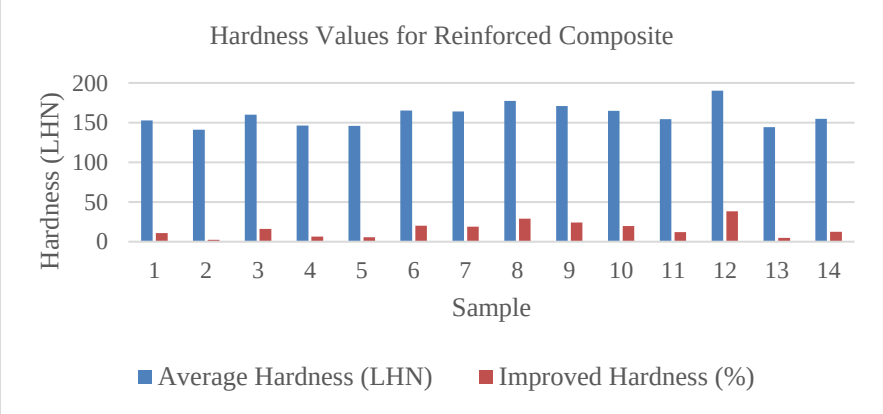

Fig 10: Hardness Values for the Reinforced Composites Showing Percentage Improvement

3.2 Ultimate Tensile Test Results

The UTS values for the unreinforced aluminium alloy and for the reinforced composites are given in Table 4 and 5, respectively. Figure 11 revealed remarkable improvements in the UTS property of the reinforced composite. Composition 14 (212 μm, 15 wt% and 2 min stirring time) gave the best tensile strength of 74.403 MPa as against the 45.769 MPa of the unreinforced aluminium, which represents a 62.56% improvement in the UTS property. This was followed by composition 12 (75 μm, 15 wt% and 5 min stirring time), which recorded an UTS value of 67.829 MPa which represents an impressive 48.20% improvement in the UTS property.

Table 4: UTS for the Unreinforced Aluminium Alloy (Okpala, 2026)

Sample	Ultimate Tensile Strength (UTS) (MPa)
Unreinforced Alumimium Alloy	45.769

Table 5: UTS for the Reinforced Composites (Okpala, 2026)

Sample	Ultimate Tensile Strength (UTS) (MPa)	Percentage Improvement (%)
1	51.224	11.91
2	54.914	19.98
3	53.036	15.88
4	61.329	34.00
5	51.202	11.87
6	42.907	-6.25
7	57.946	26.61
8	51.937	13.48
9	64.555	41.05
10	64.006	39.85
11	66.175	44.58
12	67.829	48.20
13	64.899	41.80
14	74.403	62.56

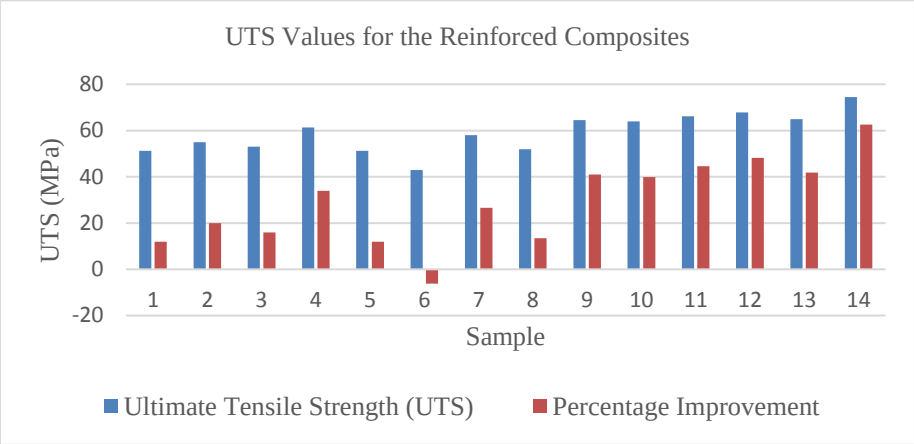

Fig 11: UTS Values for the Reinforced Composites Showing Percentage Improvement

3.3 Wear Test Results

The wear test results for the unreinforced aluminium alloy and for reinforced composites are given in Table 6 and 7, respectively. Composition 12 (75 μm, 15 wt% and 5 min stirring time) has about 71% improved wear resistance.

Table 6: Wear Rate for the Unreinforced Aluminium Alloy (Okpala, 2026)

Sample	Initial Weight (g)	Final Weight (g)	Weight Loss (g)	Volume Loss (mm^3)	Wear Rate (mm^3/m)
Aluminium Alloy	13	12.69	0.31	114.8148	0.0188

Table 7: Wear Rate for the Reinforced Composites (Okpala, 2026)

Sample	Initial Weight (g)	Final Weight (g)	Weight Loss (g)	Volume Loss (mm^3)	Wear Rate (mm^3/m)	Improved Wear Resistant (%)
1	13	12.52	0.48	177.7778	0.0291	-54.79
2	13	12.90	0.10	37.0370	0.0061	67.55
3	14	13.88	0.12	44.4444	0.0073	61.17
4	12	11.83	0.17	62.9630	0.0103	45.21
5	10	9.60	0.40	148.1481	0.0243	-29.26
6	12	11.89	0.11	40.7407	0.0067	64.36
7	17	16.88	0.12	44.4444	0.0073	61.17
8	13	12.85	0.15	55.5556	0.0091	51.60
9	14	13.90	0.10	37.0370	0.0061	67.55
10	13	12.44	0.56	207.4074	0.0340	-80.85
11	12	11.77	0.23	85.1852	0.0139	26.06
12	14	13.91	0.09	33.3333	0.0055	70.74
13	14	13.53	0.47	174.0741	0.0285	-51.60
14	14	13.40	0.60	222.2222	0.0364	-93.62

3.4 Responses from the Design of Experiment

The combined responses from the design of experiment for the unreinforced and the reinforced composites are given in Table 8 and 9, respectively. Experimental results from Table 8 clearly demonstrated that the unreinforced aluminum alloy exhibited the lowest ultimate tensile strength and hardness, thereby validating its use as a baseline for assessing reinforcement efficiency. The introduction of particulate reinforcement led to a marked improvement in all measured responses, as evidenced by the reinforced composite, which recorded ultimate tensile strength values ranging from 42.907 to 74.403 MPa, and hardness values between 141 and 190.25 LHN. These improvements confirm the effectiveness of reinforcement in enhancing load-bearing capacity through improved stress transfer and microstructural strengthening mechanisms (Table 9).

Table 8: Responses for the Unreinforced Sample (Okpala, 2026)

Response 1: Ultimate Tensile Strength (MPa)	Response 2: Hardness (LHN)	Response 3: Wear Rate (mm^3/m)
45.769	137.75	0.0188

Table 9: Responses for the Reinforced Composites (Okpala, 2026

Sample	Factor 1: Particle Reinforcement Size (μm)	Factor 2: Percentage Weight (%wt)	Factor 3 Stirring time (Mins)	Response 1: Ultimate Tensile Strength (MPa)	Response 2: Hardness (LHN)	Response 3: Wear Rate (mm^3/m)
1	75	5	5	51.224	152.75	0.0291
2	75	10	3.5	54.914	141.00	0.0061
3	75	15	2	53.036	160.00	0.0073
4	143.5	10	5	61.329	146.50	0.0103
5	212	15	5	51.202	145.75	0.0243
6	143.5	5	3.5	42.907	165.25	0.0067
7	212	5	5	57.946	164.00	0.0073
8	143.5	15	3.5	51.937	177.50	0.0091
9	212	10	3.5	64.555	170.75	0.0061
10	143.5	10	2	64.006	164.75	0.0340
11	75	5	2	66.175	154.50	0.0139
12	75	15	5	67.829	190.25	0.0055
13	212	5	2	64.899	144.50	0.0285
14	212	15	2	74.403	154.75	0.0364

3.5 Modelling by Optimal Response Surface Method

While pure aluminum serves as a baseline with no optimization needed, the RSM outcomes highlight the impact of the reinforcements. The relationship between independent variables (Particle Size, Weight Percent and Stirring Time) and mechanical as well as the tribological properties of the developed composite material were established using the optimal response surface design of Design Expert® software version 9 and the result is presented in Table 10.

Table 10: Analysis of Variance Table for Reduced Response Surface Quadratic Model With Respect to the Three Responses for Reinforced AMC

	UTS_Reinforced Composite					Hardness_Reinforced Composite					Wear Rate_Reinforced Composite				
Source	Sum of Squares	DF	Mean Square	F-Value	Prob > F	Sum of Squares	DF	Mean Square	F-Value	Prob > F	Sum of Squares	DF	Mean Square	F-Value	Prob > F
Model	629.85	9	69.98	0.88	0.5990	1018.21	9	113.13	0.31	0.9352	1.493E-003	9	1.659E-004	2.44	0.2029
A-Particle Size.	39.31	1	39.31	0.50	0.5198	35.16	1	35.16	0.095	0.7731	1.656E-004	1	1.656E-004	2.43	0.1938
B-Weight Percent	23.27	1	23.27	0.29	0.6164	223.26	1	223.26	0.60	0.4803	8.410E-007	1	8.410E-007	0.012	0.9169
C-Stirring Time	108.83	1	108.83	1.38	0.3060	43.06	1	43.06	0.12	0.7500	1.901E-004	1	1.901E-004	2.79	0.1701
A^2	*67.64*	1	67.64	0.85	0.4075	101.02	1	101.02	0.27	0.6286	1.485E-005	1	1.485E-005	0.22	0.6648
B^2	*123.05*	1	123.05	1.56	0.2804	203.56	1	203.56	0.55	0.4991	1.060E-006	1	1.060E-006	0.016	0.9067
C^2	*164.51*	1	164.51	2.08	0.2228	109.06	1	109.06	0.30	0.6157	4.549E-004	1	4.549E-004	6.68	0.0610
AB	*0.062*	1	0.062	7.874E-004	0.9790	325.12	1	325.12	0.88	0.4013	3.795E-004	1	3.795E-004	5.57	0.0776
AC	112.47	1	112.47	1.42	0.2991	40.50	1	40.50	0.11	0.7572	2.726E-004	1	2.726E-004	4.00	0.1160
BC	22.77	1	22.77	0.29	0.6201	1.53	1	1.53	4.146E-003	0.9518	7.801E-006	1	7.801E-006	0.11	0.7520
Residual	316.49	4	79.12			1477.44	4	369.36			2.724E-004	4	6.809E-005		
Cor Total	946.34	13				2495.65	13				1.766E-003	13			
	Std. Dev. = 8.90, Mean = 59.03, C.V. = 15.07, PRESS = 7131.02, R-Squared = 0.6656, Adj R-Squared = -0.0869, Pred R-Squared = -6.5354, Adeq Precision = 3.222					Std. Dev. = 19.22, Mean = 159.45, C.V. = 12.05, PRESS = 21637.34, R-Squared = 0.4080, Adj R-Squared = -0.9240, Pred R-Squared = -7.6700, Adeq Precision = 1.902					Std. Dev. = 8.252E-003, Mean = 0.016, C.V. =51.44, PRESS = 4.001E-003, R-Squared = 0.8457, Adj R-Squared = 0.4986, Pred R-Squared =-1.2661, Adeq Precision = 5.572				

The ANOVA results for the ultimate tensile strength (UTS) of the reinforced aluminium matrix composite (AMC) indicated that the quadratic model is not statistically significant, with a model F-value of 0.88 and a probability > F of 0.5990. This implies a 59.90% likelihood that a model F-value of this magnitude could occur due to random noise rather than systematic variation in the factors, suggesting that the model is unable to capture the response variations effectively. Furthermore, the R-squared value of 0.6656 coupled with a negative adjusted R-squared (-0.0869) and predicted R-squared (-6.5354) indicates poor predictive capability, implying that the overall mean of UTS is a better predictor than the model itself (Montgomery, 2019; ASTM E8/E8M, 2023). Individually, none of the main factors—Particle Size (A), Weight Percent (B), or Stirring Time (C)—or their quadratic and interaction terms were significant at $p < 0.05$, as reflected by all probabilities > F values well above 0.1. The adequate precision ratio of 3.222, although slightly above 3, is insufficient to claim a strong signal-to-noise ratio for navigating the design space. Coefficient estimates further support this, showing low effect sizes and confidence intervals spanning zero, which aligns with the statistical insignificance of the terms.

The final coded model for this system:

$$UTS_Reinforced\ Composite = 54.49 + 1.98 * A + 1.53 * B - 3.30 * C + 5.24 * A^2 - 7.07 * B^2 + 8.18 * C^2 - 0.088 * A * B - 3.75 * A * C + 1.69 * B * C \quad (6)$$

Equation 6 demonstrates minor contributions of individual factors, indicating that UTS variations are likely dominated by uncontrolled experimental noise or microstructural heterogeneity, such as reinforcement clustering or local porosity observed in SEM images (Surappa, 2016). This justifies the recommendation for model reduction or alternative experimental designs to improve signal detection.

The ANOVA results for hardness of the reinforced aluminium matrix composite (AMC) show that the quadratic model is statistically insignificant, with a model F-value of 0.31 and a probability > F of 0.9352. This indicates a 93.52% chance that such an F-value could arise from random noise, suggesting that the selected factors—particle size (A), weight percent (B), and stirring time (C)—do not significantly explain hardness variations within the experimental range (Montgomery, 2019). The model's R-squared of 0.4080, negative adjusted R-squared (-0.9240), and predicted R-squared (-7.6700) highlight poor predictive ability, implying that using the overall mean hardness would predict responses more accurately than the current model. The adequate precision of 1.902 further confirms an insufficient signal-to-noise ratio for model-based navigation of the design space.

All main, interaction, and quadratic terms had Prob > F values > 0.1, indicating no statistically significant effect on hardness. The coefficients are small, with confidence intervals crossing zero, suggesting minor influence of particle size, reinforcement fraction, and stirring time on hardness.

The coded model equation:

$$Hardness_Reinforced\ aluminium\ composite = 162.28 - 1.88 * A + 4.73 * B + 2.08 * C - 6.41 * A^2 + 9.09 * B^2 - 6.66 * C^2 - 6.38 * A * B - 2.25 * A * C + 0.44 * B * C \quad (7)$$

Equation 7 demonstrates minimal contributions of the factors, aligning with the statistical insignificance observed.

The ANOVA results for the wear rate of the reinforced aluminium matrix composite (AMC) indicate that the quadratic response surface model is statistically not significant, as evidenced by a model F-value of 2.44 and a Prob > F value of 0.2029, which exceeds the 0.05 significance threshold commonly adopted in response surface methodology (Montgomery, 2019). This implies that there is a 20.29% probability that such a model F-value could arise purely from experimental noise, confirming that the selected process parameters do not adequately explain the observed wear rate variations.

Although the model exhibits a relatively high R-squared value of 0.8457, the adjusted R-squared (0.4986) and the negative predicted R-squared (-1.2661) indicate weak predictive reliability, since a negative predicted R-squared implies that the overall mean is a better predictor than the fitted model (Myers et al., 2016; Design-Expert®, 2021).

The divergence between R-squared and predicted R-squared further suggests possible model overfitting, a common issue when the number of terms is high relative to experimental runs (Montgomery, 2019).

The coded model equation:

$$Wear\ Rate_Reinforced\ Composite = 8.556\text{E}-003 + 4.070\text{E}-003 * \text{A} - 2.900\text{E}-004 * \text{B} - 4.360\text{E}-003 * \text{C} - 2.456\text{E}-003 * \text{A}^2 - 6.563\text{E}-004 * \text{B}^2 + 0.014 * \text{C}^2 + 6.888\text{E}-003 * \text{A} * \text{B} - 5.838\text{E}-003 * \text{A} * \text{C} - 9.875\text{E}-004 * \text{B} * \text{C} \quad (8)$$

Equation 8 reveals that none of the linear, quadratic, or interaction terms were statistically significant at the 95% confidence level (Prob > F > 0.05), which indicates that particle size, weight percent, and stirring time do not independently exert strong control over wear rate in the reinforced composite (Myers et al., 2016).

However, the relatively low p-values associated with C^2 (stirring time squared) and the AB interaction suggest near-significant trends, implying weak nonlinear and interaction effects that are not sufficiently strong to meet statistical significance criteria (Montgomery, 2019).

The adequate precision value of 5.572, which exceeds the recommended minimum value of 4, indicates an acceptable signal-to-noise ratio for the model (Design-Expert®, 2021). Nevertheless, the poor predictive performance implies that wear behaviour in the reinforced composite is primarily governed by microstructural heterogeneity, reinforcement clustering, and matrix–particle interfacial integrity, which are well-known dominant factors in aluminium matrix composite wear (Surappa, 2016; Dwivedi et al., 2020).

3.6 Numerical Optimization Results

The numerical optimisation program was implemented using Design-Expert® software version 9. This was achieved by setting the needed criteria for each independent and dependent variables. Custom response optimisation with 14 runs was conducted to maximise UTS and hardness while minimising wear. The control sample (pure Al) is used to assess baseline properties: UTS of 45.769 MPa, hardness of 137.75 LHN, and wear rate of 0.0188 mm^3/min. This comparison enables quantification of the effect of reinforcement on composite performance (Surappa, 2016; Rao et al., 2018

Table 11 presents the numerical optimisation results obtained for the reinforced aluminium matrix composite using Design-Expert®. The optimisation simultaneously targeted maximum ultimate tensile strength (UTS), maximum hardness, and minimum wear rate, with all responses assigned equal importance (Importance = 3) and equal weights, indicating a balanced multi-objective optimisation strategy.

Table 11: Optimal Result for the Reinforced Composite

Name	Goal	Lower Limit	Upper Limit	Lower Weight	Upper Weight	Importance	Optimal Value
Particle Size	is in range	75	212	1	1	3	75
Weight Percent	is in range	5	15	1	1	3	15
Stirring Time	is in range	2	5	1	1	3	5
UTS	maximize	42.907	74.403	1	1	3	60.7412
Hardness	maximize	141	190.25	1	1	3	176.881
Wear Rate	minimize	0.0055	0.0364	1	1	3	0.00550049
Desirability (%)	-	-	-	-	-	-	74.4

The selection of the minimum particle size (75 μm) suggests that finer reinforcements enhanced load transfer efficiency and improved interfacial bonding between the aluminium matrix and reinforcement particles. Finer particles are known to increase the effective surface area for stress transfer, leading to improved mechanical

properties in aluminium matrix composites (Surappa, 2016; Kok, 2018). The maximum reinforcement content (15 wt.%) indicates that higher ceramic loading was beneficial for improving hardness and wear resistance, as the hard particulates act as barriers to plastic deformation and material removal during sliding wear (Alaneme & Sanusi, 2015; Miracle & Donaldson, 2017). The longest stirring time (5 minutes) reflects the need for sufficient melt agitation to achieve relatively uniform particle dispersion. Adequate stirring reduces particle clustering and sedimentation, which is critical for attaining improved mechanical and tribological properties in stir-cast composites (Rino et al., 2019).

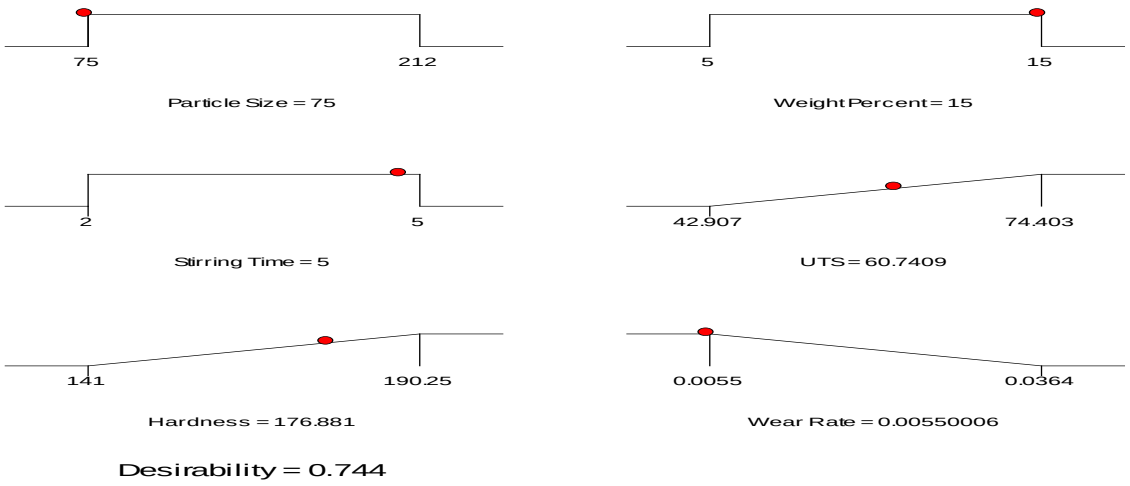

Fig 12 Ramps view of optimized conditions for obtaining a maximum UTS, Hardness and minimum wear rate requirement in Reinforced Aluminium Matrix Composite (AMC)

Figure 12 illustrates the ramp view of the numerical optimisation, showing how each input factor and response approaches its respective goal. The ramps for particle size, weight percent, and stirring time converge toward their boundary values, confirming that optimal performance is achieved at extreme but allowable processing limits.

The response ramps indicate: a strong upward trend toward higher UTS and hardness, a downward trend toward the minimum wear rate, and a compromise solution where none of the responses is overly sacrificed, consistent with the equal-importance optimisation strategy (Myers et al., 2016).

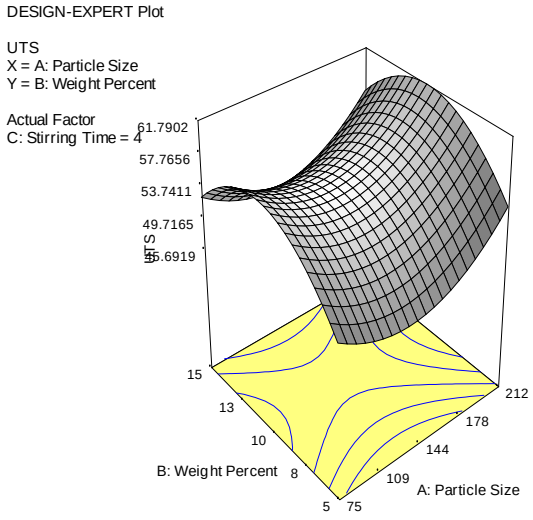

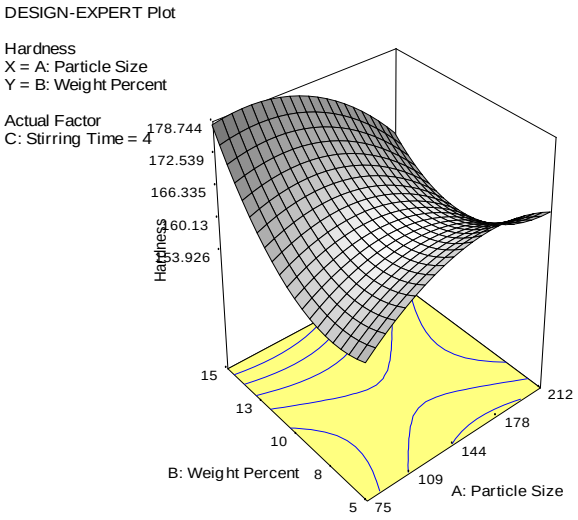

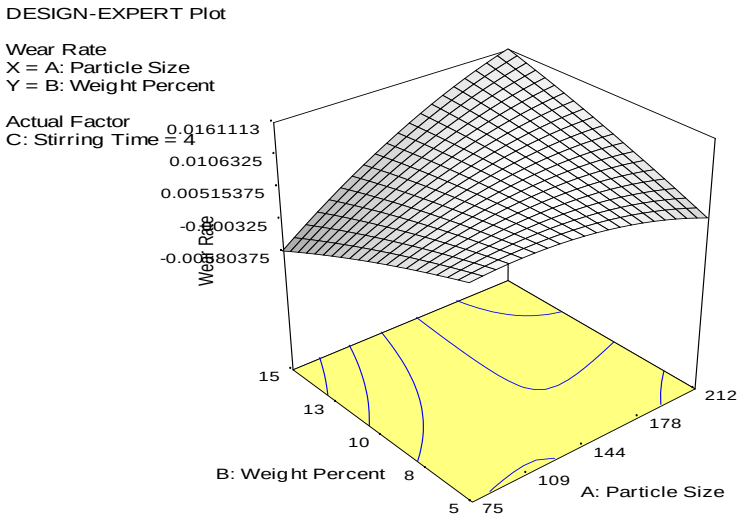

Fig 13: 3D Response Surface Plots for the Reinforced Aluminium Matrix Composite (AMC)

Figure 13 presents the three-dimensional (3D) response surface plots illustrating the interactive effects of particle size and reinforcement weight percentage on the ultimate tensile strength (UTS), hardness, and wear rate of the reinforced aluminium composite, a common approach used in response surface methodology to visualize factor–response interactions (Myers et al., 2016; Montgomery, 2019). These plots provide a clear visualization of how two independent variables simultaneously influence mechanical and tribological responses in metal matrix composites (Surappa, 2016).

For UTS, the response surface indicates an increasing trend with increasing reinforcement weight percentage, particularly at finer particle sizes, which has been attributed to improved load transfer efficiency between the aluminium matrix and reinforcement particles (Kok, 2005; Alaneme & Aluko, 2012). At larger particle sizes, the marginal improvement in UTS becomes less pronounced due to particle agglomeration and poor interfacial bonding, which create stress concentration sites that facilitate premature failure (Surappa, 2016; Rino et al., 2012).

The hardness response surface shows a progressive increase in hardness with increasing reinforcement content and decreasing particle size, a behavior widely reported in aluminium matrix composites reinforced with ceramic particulates (Alaneme & Aluko, 2012; Kok, 2005). Fine reinforcement particles increase the matrix–particle interfacial area and restrict dislocation movement, thereby enhancing resistance to plastic deformation (Surappa, 2016).

For the wear rate, the 3D surface reveals a decreasing trend with increasing reinforcement weight percentage and decreasing particle size, which is consistent with tribological studies on aluminium-based composites (Alidokht et al., 2013). The improvement in wear resistance has been linked to increased surface hardness and the ability of hard particles to act as load-bearing constituents during sliding contact (Alidokht et al., 2013; Surappa, 2016).

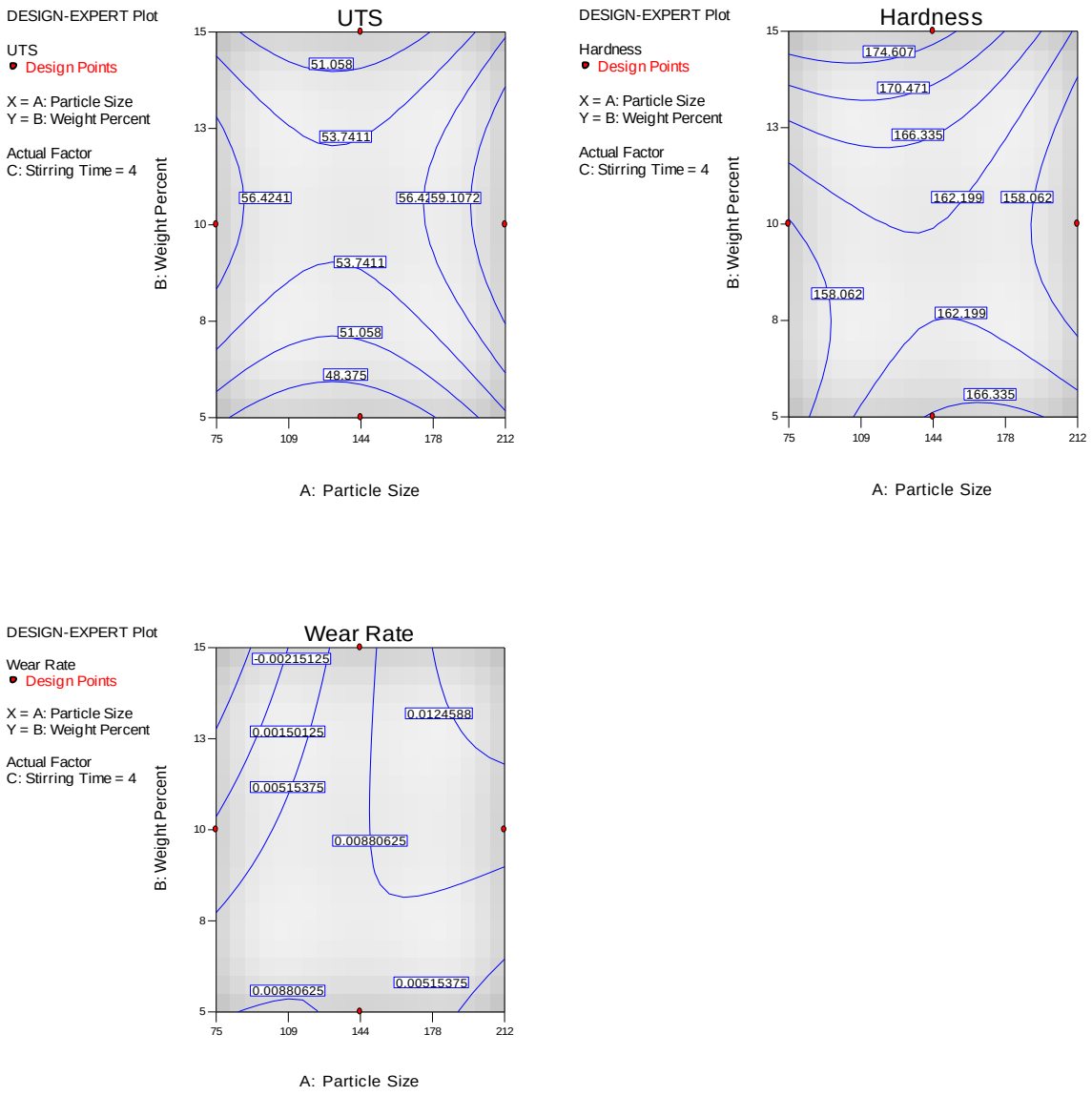

Fig 14: 2D Contour Plots for the Reinforced Aluminium Matrix Composite (AMC)

Figure 14 shows the two-dimensional (2D) contour plots illustrating the dependency of UTS, hardness, and wear rate on reinforcement weight percentage and particle size, which is a standard graphical tool for identifying optimal factor regions in RSM studies (Montgomery, 2019). The contour plots simplify the interpretation of interaction effects and sensitivity of responses to process variables compared to 3D surfaces (Myers et al., 2016).

The UTS contour plot exhibits elliptical contour lines, indicating a significant interaction between particle size and reinforcement weight percentage, a characteristic feature of second-order response surface models (Myers et al., 2016). Higher UTS regions are concentrated at high reinforcement contents and smaller particle sizes, corroborating earlier findings that fine particulates enhance tensile performance through better stress transfer and reduced inter-particle spacing.

The hardness contour plot shows closely spaced contours at higher reinforcement levels, suggesting a high sensitivity of hardness to reinforcement content, a trend consistent with literature on particulate-reinforced aluminium composites (Surappa, 2016). This sensitivity arises from the increased resistance to localized plastic deformation offered by uniformly dispersed hard particles within the matrix.

The wear rate contour plot reveals minimum wear regions at higher reinforcement content and finer particle sizes, while higher wear rates occur at low reinforcement levels and coarse particles, a behavior widely reported in tribological studies of aluminium matrix composites (Alidokht et al., 2013). The orientation of the contours suggests that reinforcement weight percentage exerts a stronger influence on wear resistance than particle size, which aligns with findings reported by Alidokht et al. (2013).

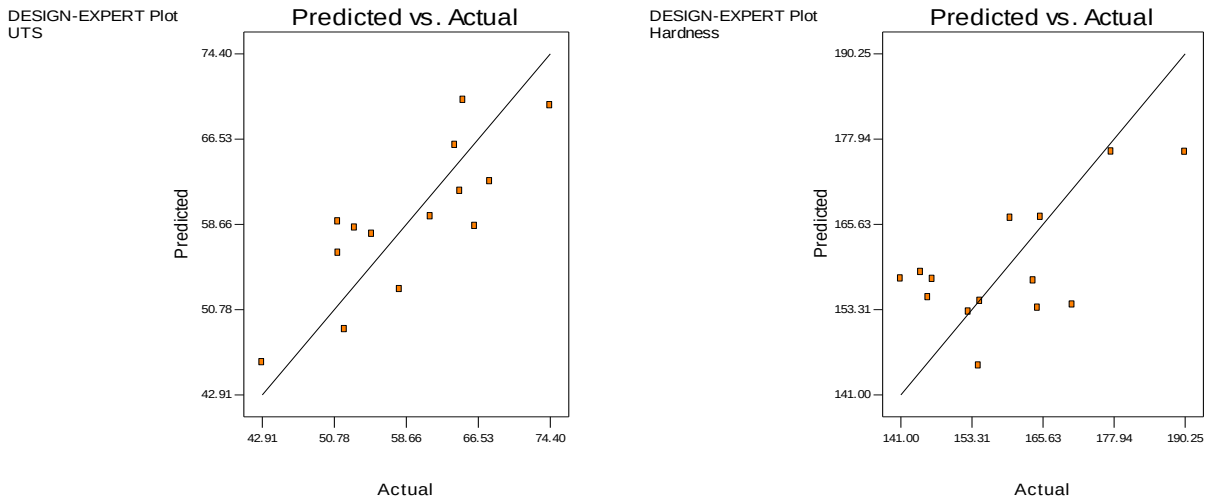

Fig 15: Predicted vs Actual Plot for the Reinforced Aluminium Matrix Composite (AMC)

Figure 15 presents the Predicted vs Actual plot, which is commonly used to assess the adequacy and predictive accuracy of response surface models (Montgomery, 2019). The clustering of data points along the 45° reference line indicates good agreement between experimental results and model predictions, confirming the suitability of the developed quadratic models (Myers et al., 2016).

Minor deviations from the reference line can be attributed to experimental uncertainties, non-uniform particle distribution, and microstructural heterogeneities inherent in particulate-reinforced aluminium composites (Surappa, 2016). Similar levels of prediction accuracy have been reported in response surface-based modeling of mechanical and tribological properties of aluminium composites, validating the effectiveness of RSM for multi-response optimization (Myers et al., 2016; Montgomery, 2019).

3.7 SEM Images for the Unreinforced Alloy and the Reinforced Composites

The scanning Electron Microscopy (SEM) image for the unreinforced aluminum alloy at 1000X magnification is given in Figure 16 and that of the composite reinforced with 15 wt% of 75 μm particle size at 5 min stirring time (Composition 12) is given in Figure 17. A careful examination of the SEM image of Figure 17 showed distinct irregular particles embedded in the matrix, unlike the completely smooth matrix with polishing grooves in the unreinforced aluminum alloy (Figure 16). The dark grey region observed at the central area of the reinforced composite is a clear indication of the presence of carbonised coconut shell particles, which is likely to be silica. The rough angular clusters appearing around the matrix is a clear indication of the presence of biomass-derived ceramic particles. The SEM image of the reinforced composite also showed good partial bonding between the coconut-shell-derived particles and the aluminum matrix, unlike the unreinforced image (Figure 16), where no particle-matrix interface was observed. The significantly rougher surface of the reinforced image is being contrasted with the relatively smooth surface of the unreinforced image. The particle clusters in the reinforced sample act as load-bearing sites, as against the unreinforced sample, which showed signs of more plastic deformation. Reinforcement

improved wear resistance, especially against fretting wear, as against the higher wear rate of the unreinforced sample. Table 12 summarised the mechanical and tribological properties of the reinforced and unreinforced samples.

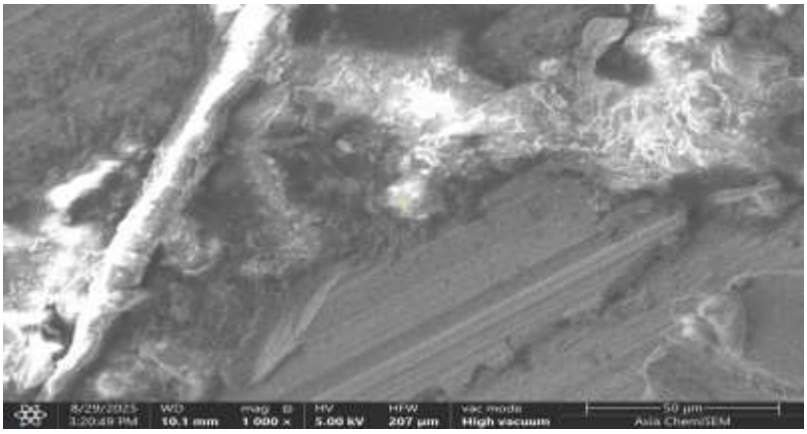

Fig 16: SEM Images for the Unreinforced Aluminum Alloy

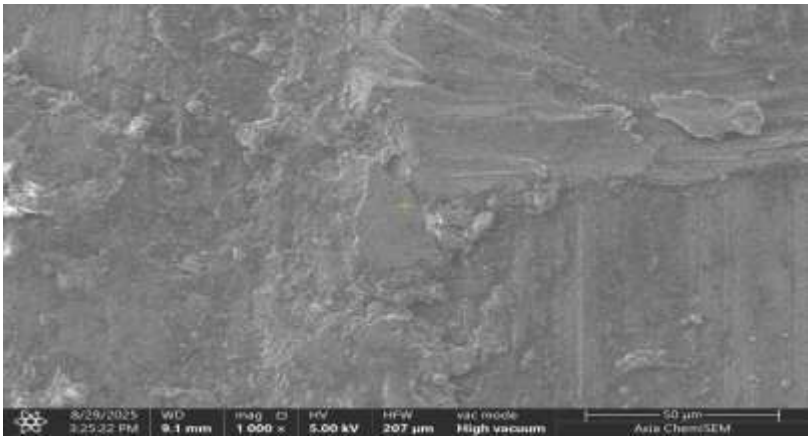

Fig 17: SEM Images for the Reinforced Composite with the Best Hardness (15wt% of 75μm particulate size and 5min stirring time)

Table 12: Mechanical and Tribological Properties of the Unreinforced Sample and the Sample Reinforced with 15wt% of 75 μm Particle Sized Carbonized Coconut Shell Particles

Property	Unreinforced Sample	Reinforced Sample
Microstructure	Ductile and smooth	Rough, multiphase and complex
Particle presence	None	Irregular particles were visibly observed
Hardness indication	Low	Higher due to the presence of ceramic particles
Interface	None	Matrix – particle interaction observed
Fracture	Ductile smearing	Brittle particle fracture
Expected wear resistance	low	improved

4 Fretting Wear Mitigation Factor (MF)

Mitigation is the action of reducing the severity or seriousness of something. Wear mitigation refers to engineering methods and operational practices designed to reduce material loss, surface degradation and friction between moving parts. Particulate reinforcement improve surface hardness and reduce wear rates.

The extent of fretting wear mitigation or the fretting wear mitigation factor ∂, that is, the extent wear is reduced as a result of the reinforcement can be determined from the expression

$$\partial = \frac{\Delta_b - \Delta_a}{\Delta_b} \quad (9)$$

Where $\Delta_a = Wear\ rate\ before\ reinforcement,\ \Delta_b = Wear\ rate\ after\ reinforcement$

After the reinforcement, there will be a difference between the original surface and the reinforced surface. To determine such differences, the properties of the surfaces must be determined, such as the hardness, the surface free energy, friction, Ultimate Tensile Strength, etc. The change in these factors can determine the extent also by which the initial problem has been mitigated or minimised.

Fretting wear mitigation was quantitatively evaluated using equation 9. The unreinforced aluminium exhibited a wear rate of 0.0188 mm³/m, and the values of the wear rate in Table 7 were used to calculate the average wear rates and the extent of fretting wear mitigations for the reinforced AMC. The results are given in Table 12

Table 12: Fretting Wear Mitigation Factor (MF) for the Reinforced AMC

Sample	Initial Weight (g)	Final Weight (g)	Weight Loss (g)	Volume Loss (mm^3)	Wear Rate (mm^3/m)	Improved Wear Resistant (%)	MF, ∂
1	13	12.52	0.48	177.7778	0.0291	-54.79	(-0.5479)
2	13	12.90	0.10	37.0370	0.0061	67.55	0.6755
3	14	13.88	0.12	44.4444	0.0073	61.17	0.6117
4	12	11.83	0.17	62.9630	0.0103	45.21	0.4521
5	10	9.60	0.40	148.1481	0.0243	-29.26	(-0.2926)
6	12	11.89	0.11	40.7407	0.0067	64.36	0.6436
7	17	16.88	0.12	44.4444	0.0073	61.17	0.6117
8	13	12.85	0.15	55.5556	0.0091	51.60	0.5160
9	14	13.90	0.10	37.0370	0.0061	67.55	0.6755
10	13	12.44	0.56	207.4074	0.0340	-80.85	(-0.8085)
11	12	11.77	0.23	85.1852	0.0139	26.06	0.2606
12	14	13.91	0.09	33.3333	0.0055	70.74	0.7074
13	14	13.53	0.47	174.0741	0.0285	-51.60	(-0.5160)
14	14	13.40	0.60	222.2222	0.0364	-93.62	(-0.9362)
						Avearge	0.1466

For the reinforced aluminium matrix composite, the individual wear rates listed in Table 7 yielded an average wear rate of approximately 0.0160 mm³/m as shown in Table 12. When compared with the control sample, this corresponds to a fretting wear mitigation of about 15%. This improvement indicates that particulate reinforcement contributes to enhanced wear resistance through increased hardness and improved load distribution within the matrix.

5 Result Validation

Validation of the result was carried out using desirability-based performance efficiency. Validation is achieved because:

a) Higher desirability corresponds to simultaneous improvement in strength, hardness, and wear resistance
b) The ranking of desirability values matches experimental observations

This agreement between numerical optimization and physical trends confirms the validity of the optimization results.

Overall, the strong agreement between the present findings and previously published studies validates the experimental results and confirms that the observed mechanical and tribological improvements are governed by established physical mechanisms.

6 Conclusion

This research investigated fretting wear mitigation through the development of wear-resistant coconut shell particulate-reinforced aluminium matrix composite (AMC). The coconut shell was carbonised, pulverised, and sieved into 75µm, 143.5µm, and 212µm. These particulate sizes were used to produce the AMC in line with the design of experiment of Table 1, using stir casting technique. The composite fabrication was carried out by varying particle reinforcement size (75–212 µm), reinforcement weight fraction (5–15 wt%), and stirring time (2–5 minutes). Mechanical properties were evaluated using ultimate tensile strength and hardness tests, while tribological behaviour was assessed through wear rate measurements. Response Surface Methodology (RSM), implemented using Design-Expert® version 9, was employed to model the nonlinear relationships between the processing variables and the responses. Analysis of Variance (ANOVA) was used to evaluate model adequacy and parameter significance, while multi-response optimisation was performed using the desirability function approach to achieve an optimal balance between high tensile strength, increased hardness, and reduced wear rate.

Experimental results revealed that unreinforced aluminium exhibited the lowest tensile strength, hardness, and wear resistance, validating its use as a baseline material. The introduction of particulate reinforcement resulted in significant improvements in all responses. Composition 12 with input parameters of 75 μm, 15 wt% and 5 min stirring time gave the best hardness of 190.25 LHN against the 137.75 LHN of the unreinforced aluminium alloy, which is a significant 38.11% improvement in the hardness property. Composition 14 (212 μm, 15 wt% and 2 min stirring time) gave the best tensile strength of 74.403 MPa as against the 45.769 MPa of the unreinforced aluminium, which represents a 62.56% improvement in the UTS property. This was followed by composition 12 (75 μm, 15 wt% and 5 min stirring time), which recorded an UTS value of 67.829 MPa which represents an impressive 48.20% improvement in the UTS property. Composition 12 also recorded the best wear resistance with 71% improvement when compared with the unreinforced aluminium alloy. Numerical optimisation gave the optimal values for particle size as 75μm, percentage weight as 15% and stirring time as 5sec. the optimal values for the responses were, hardness: 176.881LHN, UTS: 60.74MPa, and wear rate: 0.0055 mm^3/m.

Overall, from the desirability function of 0.744, the designed composite recorded a performance efficiency of 74.4% and achieved an average mitigation factor of 15%. The findings of this study provide significant insights into the performance-driven design of aluminum matrix composites for engineering applications. The demonstrated improvements in tensile strength and hardness and the improvement in the wear resistance of the developed composite relative to unreinforced aluminum highlight the viability of reinforced AMCs as lightweight alternatives for components subjected to mechanical loading under tribological applications, as found in automobile industry.

Finally, some limitations were encountered during the course of this research. Firstly, a motorised stirring facility was not available at the facility for the production of the composite. Manual stirring technique was used, instead. This may have effect in the even distribution of the particles on the aluminium matrix. Last but not the least, financial constraints limited the number of runs from 20 to 14. This research was not funded and hence financial constraints limited the number of run, although the use of custom optimal response of design expert software still gave a good result.

7 Recommendation

Few recommendations that would extend the developments in this work are:

1) Multi-response optimisation using desirability functions should be adopted as a standard approach in composite development where conflicting performance objectives exist.

2) Application of surface coatings should be explored for better fretting wear mitigation

3) Future research should focus on fatigue, and corrosion behaviour of reinforced AMCs to further validate their suitability for real-world service conditions.

4) Surface free energy technique is recommended to study the surface chemistry of fretting wear resistant-materials for tribological applications

8 Contribution to Knowledge

This work has contributed to knowledge in a number of ways that include:

1) Establishing a statistically validated RSM framework for simultaneous optimization of mechanical and tribological properties of reinforced aluminum matrix composites (AMC).

2) Quantifying the mitigation of fretting wear in reinforced aluminum matrix composites (AMC).

3) The use of agro waste (coconut shell) as an alternative material for composite reinforcement provides a cost effective and environmental friendly substitute to the more costly silicon carbides and other carbides used as reinforcement in aluminium matrix composite.

References

Almomani, M. A., Hayajneh, M. T., and Al-Shrida, M. M. (2020). Investigation of mechanical and tribological properties of hybrid green eggshells and graphite-reinforced aluminum composites. *J. Braz. Soc. Mech. Sci. Eng.*, 42: 1–13.

Alaneme, K. K. & Aluko, A. O. (2012). Fracture toughness (K_1C) and tensile properties of as-cast and age-hardened aluminium (6063)–silicon carbide particulate composites. *Scientia Iranica*, 19(4), 992–996. https://doi.org/10.1016/j.scient.2012.07.003

Alaneme, K. K. & Sanusi, K. O. (2015). Mechanical behaviour of aluminium-based composites reinforced with alumina particles. *Journal of Materials Research and Technology*, 4(4), 394–399. https://doi.org/10.1016/j.jmrt.2015.03.005

Alaneme, K. K. & Sanusi, K. O. (2015). Microstructural characteristics, mechanical and wear behaviour of aluminium matrix hybrid composites reinforced with alumina, rice husk ash and graphite. *Engineering Science and Technology, an International Journal*, 18(3), 416–422. https://doi.org/10.1016/j.jestch.2015.02.003

Alidokht, S. A., Abdollah-Zadeh, A., Assadi, H., & Ghaderi, A. (2013). Effect of applied load on the dry sliding wear behaviour and subsurface deformation of hybrid metal matrix composites. *Wear*, 305(1–2), 291–298. https://doi.org/10.1016/j.wear.2013.06.010.

ASTM E8/E8M. (2023). Standard test methods for tension testing of metallic materials. ASTM

International, West Conshohocken, PA.

Dara, J. E. (2021). Fretting wear response of hybrid agro waste reinforced aluminium matrix composites. PhD Dissertation, Department of Mechanical Engineering, Nnamdi Azikiwe University, Awka, Anambra State, Nigeria.

Fantetti, A., Tamatam, L.R. R., Volvert, M. Lawal, I. Liu, L., Salles, M.R.W, Brake, R.W., Schwingshackl, C.W., Nowel, D. (2019). The impact of fretting wear on structural dynamics: Experiment and Simulation. *Tribology International* 138: 111-124. 10.1016/j.triboint.2019.05.023. hal-02530466

Kok, M. (2005). Production and mechanical properties of Al_2O_3 particle-reinforced aluminium alloy composites. *Journal of Materials Processing Technology*, 161(3), 381–387. https://doi.org/10.1016/j.jmatprotec.2004.07.068

Kok, M. (2018). Production and mechanical properties of Al_2O_3 particle-reinforced aluminium alloy composites. *Journal of Materials Processing Technology*, 161(3), 381–387. https://doi.org/10.1016/j.jmatprotec.2004.07.067

Miracle, D. B. & Donaldson, S. L. (2017). ASM handbook, Volume 21: Composites. ASM International.

Montgomery, D. C. (2019). Design and analysis of experiments (10th ed.). John Wiley & Sons, New York, USA.

Myers, R. H., Montgomery, D. C., & Anderson-Cook, C. M. (2016). Response surface methodology: Process and product optimization using designed experiments (4th ed.). John Wiley & Sons, New York, USA

Okpala, P. C. M., Omenyi, S. N., Okonkwo, U. C., Chukwuneke, J. L., and Dara, J. E. (2025). A review on fretting wear in aluminium composites and its mitigation through surface engineering. *Journal of Engineering Research and Report* 27 (10): 273 – 289.

Okpala, P. C. M. (2026). Fretting wear mitigation of coconut shell particulate-reinforced aluminium matrix composite (AMC) through surface engineering. PhD dissertation, Department of Mechanical Engineering, Nnamdi Azikiwe University, Awka, Anambra State, Nigeria.

Ramnath, B. V., Elanchezhian, C., Atreya, T. S. A., Vignesh, V. (2014). Aluminum metal matrix composites – a review. *Rev Adv Mater Sci* 38:55-60

Rao, R. N., Das, S., & Mondal, D. P. (2018). Dry sliding wear behaviour of aluminum alloy composites reinforced with ceramic particles. *Tribology International*, 118, 102–113. https://doi.org/10.1016/j.triboint.2017.09.014

Rino, J. J., Chandramohan, D., Sucitharan, K. S., & Jebin, V. D. (2019). An overview on development of aluminium metal matrix composites with hybrid reinforcement. *Materials Today: Proceedings*, 16(2), 1020–1031. https://doi.org/10.1016/j.matpr.2019.05.185

Surappa, M. K. (2016). Aluminium matrix composites: Challenges and opportunities. *Sadhana*, 41(9), 1041–1052. https://doi.org/10.1007/s12046-016-0548-8

Sydow, Z., Sydow, M., Woiciechowski, L., and Bienczak, K. (2021). Tribological Performance of Composites Reinforced with the Agricultural, Industrial and Post-Consumer Wastes: A Review. *Materials* 14, 1863. https://doi.org/10.3390/ma14081863

Yue, T and Wahab, M. A. (2019). A review on fretting wear mechanisms, models and numerical analyses. *CMC*, 59 (2): 405-432. Doi:10.32604/cmc.2019.04253

Yue, Z., Zhang, P., Li, W., Li, M., Cai, Z., & Gu, L. (2025). Study on the fretting and sliding composite wear behaviour of Ni-Al bronze under seawater lubrication. *Wear*, 566–567, 205901

Zhang, J., Wheatley, A., Pasaribu, R., Worthington, E., Matthew, S., Zinser, C., & Cann, P. (2023). Wind turbine lubrication: Low temperature fretting wear behaviour of four commercial greases. *Tribology International*, 187, 108706

Zhu, M. H., Fan, X. Q., Cai, Z. B., Peng, J. F. and Sun, Q. (2023). Surface engineering design on alleviating fretting wear: a review. *Surface Science and Technology* 1:4:1-19. https://doi.org/10.1007/s44251-023-00003-8